

New approaches in Electromagnetic Compatibility / Nouvelles approches en Compatibilité
Electromagnétique
**Characterization of radiated electromagnetic fields using equivalent
sources – Application to the EMC of power printed circuit boards**

Lotfi Beghou^{a,b,*}, Lionel Pichon^a, François Costa^{b,c}

^a *Laboratoire de génie électrique de Paris (LGEP), UMR 8507 CNRS, SUPELEC, Université Paris Sud, UPMC–Université Paris 06, plateau de Moulon, 91192 Gif sur Yvette cedex, France*

^b *Laboratoire SATIE, UMR 8029, UniverSud, École normale supérieure, 94230 Cachan, France*

^c *IUFM Créteil, Université Paris 12, France*

Available online 14 March 2009

Abstract

This article presents an original methodology to characterize electromagnetic disturbances radiated from power electronic devices. The method is based on the substitution of the power device by an equivalent set of elemental dipoles (electric and magnetic dipoles). The set of dipoles radiates the same near-field. The dipoles are determined from a near field cartography of the fields obtained with a measurement bench. The dipole parameters are determined by solving an inverse problem using a genetic algorithm. The efficiency of the approach is demonstrated on an academic DC-DC converter. Finally some results about the chopper are presented. The methodology has two advantages: first it allows one to define some threshold limitations for electromagnetic fields on the surroundings and secondly it gives the location of the real source distribution. **To cite this article: L. Beghou et al., C. R. Physique 10 (2009).**

© 2009 Académie des sciences. Published by Elsevier Masson SAS. All rights reserved.

Résumé

Caractérisation des champs de rayonnements électromagnétiques en utilisant des sources équivalentes – application au CEM des cartes de circuit imprimé. Cet article présente une méthode de modélisation des rayonnements en champ proche des alimentations à découpage. Cette méthode consiste à remplacer par un ensemble de dipôles élémentaires (dipôles électriques et dipôles magnétiques) le dispositif sous test. Cet ensemble de dipôles rayonne le même champ électromagnétique que le dispositif réel. Un algorithme génétique est utilisé pour la résolution du problème inverse qui permet de trouver les paramètres du modèle. Dans ce but, des mesures de champ électromagnétique proche sont effectuées. La méthode a été appliquée au cas d'un hacheur académique. Enfin quelques résultats sur le hacheur sont présentés. **Pour citer cet article : L. Beghou et al., C. R. Physique 10 (2009).**

© 2009 Académie des sciences. Published by Elsevier Masson SAS. All rights reserved.

Keywords: Electromagnetic radiation; Printed circuit board

Mots-clés : Rayonnement électromagnétique ; Carte de circuit imprimé

* Corresponding author.

E-mail addresses: lotfi.beghou@lgep.supelec.fr, lotfi.beghou@satie.ens-cachan.fr (L. Beghou).

1. Introduction

Switched Mode Power Supplies (SMPS) are increasingly distributed throughout embedded systems. These devices are DC-DC converters and allow one to obtain good efficiency and high power-weight and power-volume ratios. However, the switching mode involves important conducted and radiated electromagnetic perturbations. Therefore, the issue of their electromagnetic compatibility (EMC) is now a crucial challenge.

The development of predicting tools is essential in order to assess any EMC troubles. A natural way to evaluate the radiated field is to exactly describe the geometry of emissive sources and to use a 3D electromagnetic model. Such an approach requires many simplifying assumptions and is limited by the complexity of the geometry. Near-field techniques constitute an efficient approach to characterize complex radiating systems. For example, in [1] the authors deduce the size and the location of an equivalent planar loop from near field cartography using the maximum values of the magnetic field. In [2] the device is substituted by a set of dipoles covering all the scan area and radiating the same magnetic field as the measured one with a given error. In [3] a genetic algorithm was proposed to study radiation from high frequency devices.

This article presents a methodology dedicated to power devices. A set of electric and magnetic dipoles deduced from near-field measurements using a near-field test bench is obtained as an equivalent model of the device. The dipoles are determined by solving an inverse problem using a Genetic Algorithm (GA). Thus a behavioural 3D model representing the real source distribution is obtained taking into account the position, the moment orientation of dipoles. The reflexion phenomena due to the ground plane are considered using the image theory. A real DC-DC converter demonstrates that the approach provides a straightforward way to obtain the radiated field in a practical case. Adequate solutions to assess radiating troubles can then be developed.

2. Characterization method

The methodology presented here aims at finding an equivalent set of elementary magnetic dipoles, which radiate the same near-field as the original device. It is an inverse problem-based resolution method. By solving the inverse problem the parameters of the equivalent radiative source are calculated. For this purpose we optimize a fitness function, which represents the distance between the measured field \vec{H}_{mes} and the theoretical one \vec{H}_{mod} . This function depends on the parameters we are looking for.

Let $J(\vec{X})$ be the fitness function, and \vec{X} be the parameter vector which characterizes the dipoles. The fitness function can be written:

$$J(\vec{X}) = \sum_{i=1}^P \|\vec{H}_{\text{mes}} - \vec{H}_{\text{mod}}\| \quad (1)$$

where P is the number of measurement points of the magnetic field.

2.1. The model

A magnetic dipole located at position \vec{s} with a radius a and a constant current I in the wire, is characterized by its magnetic moment (Fig. 1):

$$\vec{M} = I\vec{s} = I\pi a^2 \vec{u} \quad (2)$$

where \vec{u} is the unit orientation vector of the magnetic moment.

The magnetic field radiated by one magnetic dipole is given by [4]:

$$\vec{H}(\vec{R}, k) = F(\vec{R}, k) \cdot \vec{M} - G(\vec{R}, k) \cdot (\vec{M} \cdot \vec{R}) \cdot \vec{R} \quad (3)$$

where $k = 2\pi/\lambda$ is the wave number (λ is the wave length) and $\vec{R} = \vec{r} - \vec{s}$ with \vec{s} the position vector of the magnetic dipole and \vec{r} the vector defining the position of the observation point.

$$F(\vec{R}, k) = \frac{k^2}{4\pi} \left(1 + j \frac{1}{kR} - \frac{1}{(kR)^2} \right) \frac{e^{jkR}}{R} \quad (4)$$

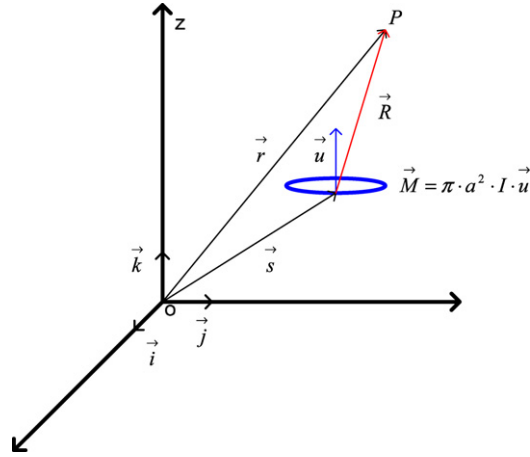


Fig. 1. Magnetic field radiated by a loop current.

$$G(\vec{R}, k) = \frac{k^2}{4\pi} \left(1 + \frac{3j}{kR} - \frac{3}{(kR)^2} \right) \frac{e^{jkR}}{R^3} \quad (5)$$

Thus for one observation point, the magnetic field can be expressed in a matrix form as follows:

$$\vec{H}(\vec{R}, k) = A(\vec{R}, k) \cdot \vec{M} \quad (6)$$

where:

$$A(\vec{R}, k) = F(\vec{R}, k) \cdot I_3 - G(\vec{R}, k) \cdot A_1(\vec{R}) \quad (7)$$

$$[A_1(\vec{R})]_{ij} = R_i R_j \quad (8)$$

The matrix A is given by (9):

$$A = \begin{bmatrix} F - GR_x^2 & -GR_x R_y & -GR_x R_z \\ -GR_y R_x & F - GR_y^2 & -GR_y R_z \\ -GR_z R_x & -GR_z R_y & F - GR_z^2 \end{bmatrix} \quad (9)$$

For P observation point \vec{R}_j , $j = 1, \dots, P$, the values of the magnetic field stand in a global vector given by:

$$\vec{H}_{\text{mod}} = \begin{bmatrix} \vec{H}(\vec{R}_1) \\ \vdots \\ \vec{H}(\vec{R}_P) \end{bmatrix} = \begin{bmatrix} A(\vec{R}_1) \\ \vdots \\ A(\vec{R}_P) \end{bmatrix} \cdot \vec{M} \quad (10)$$

The number P is a precision parameter which is inversely proportional to the measurement step. Since this step is rather small comparing to the device dimensions the measurements points are no more important and increasing them will not necessarily give better results.

With N magnetic dipoles and assuming z^i known (dipoles layed down on the PCB) the parameters vector \vec{X} is defined as:

$$\vec{X} = \begin{pmatrix} x^1 \\ y^1 \\ M^1 \\ \theta^1 \\ \phi^1 \\ \vdots \\ x^N \\ y^N \\ M^N \\ \theta^N \\ \phi^N \end{pmatrix} \left. \begin{array}{l} \left. \begin{array}{l} \text{Position of the dipole } 1^* \\ \vec{M} \text{ vector of the dipole } 1^{**} \end{array} \right\} \right\} \begin{array}{l} \text{Parameters of the dipole } 1 \\ \text{Parameters of } N \text{ dipoles} \end{array} \right.$$

* : $\|\vec{R}_{j=1...j}\| = \sqrt{(x_j - x^1)^2 + (y_j - y^1)^2 + (z_j - z^1)^2}$
 ** : $u_{M_i} = \sin(\theta_i) \cdot \cos(\phi_i) \cdot \vec{i} + \sin(\theta_i) \cdot \sin(\phi_i) \cdot \vec{j} + \cos(\theta_i) \cdot \vec{k}$

where x^i, y^i are, the dipole i center coordinates, M^i the dipole moment amplitude and θ^i, ϕ^i are the spherical angles defining the moment unit orientation vector. So in case of N dipoles the number of degrees of freedom in the fitness function J is $5 \times N$. The function J is highly nonlinear with many local minima. In order to optimize this function, a genetic algorithm is used.

2.2. Optimization

The Genetic Algorithm (GA) is a global stochastic optimization method. It simulates the evolution process of a population over the generations with specific criterion selection. Theoretically the GA has to reach the absolute optimum. Unfortunately, practical applications do not always follow the theory [5]. The main reasons are:

- There is a limit of the hypothetically unlimited number of iterations;
- There is a limit of the hypothetically unlimited population size.

To apply the GA for a problem, the following are needed:

1. The coding

It is a genetic representation of the potential solutions of the problem. The binary vector v represents one of them. The different parts of v corresponding to components of the vector \vec{X} are called *Chromosomes*. They represent the values of the studied parameters and their length depends on the required accuracy.

2. The fitness function

It evaluates the individuals and orders them according to their values.

3. The genetic operators

- Crossover

The crossover operation allows us to explore the research field. It consists on a chromosome exchange between the parents v_1, v_2 giving birth to new individuals v'_1, v'_2 . It usually follows the selection operation from which the parents v_1, v_2 are selected.

$$\begin{array}{l} v_1 = (.111|010) \\ v_2 = (.100|111) \end{array} \Rightarrow \begin{array}{l} v'_1 = (.111|111) \\ v'_2 = (.100|010) \end{array}$$

The offspring v'_1, v'_2 will take place of their parents in the new population.

- Mutation

As well as the crossover, the mutation aims at exploring the research field. It consists on the alteration of one or several genes of some individuals. For example if the individual v'_2 is selected to undergo mutation for the

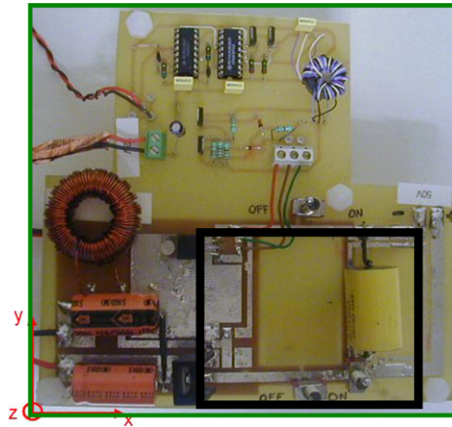


Fig. 2. Converter under test (green: scan area, black: switching cell).

third bit a new individual v_2'' will be obtained:

$$v_2' = (100111) \Rightarrow v_2'' = (101111)$$

v_2'' will take the place of v_2' .

4. Genetic parameters

- Population size N_{pop}
- Generations number N_{gen}
- Crossover probability p_c and mutation probability p_{mu} , they define the number of individuals who go under both operations.

At the end of the process we should get a population constituted of the best individuals. However, the number of dipoles is deduced after running the GA with different configurations.

3. Converter under test

Fig. 2 shows a picture of the studied converter. It is an academic Buck chopper fed by a 50V DC voltage source E . The switching frequency is $F = 20$ KHz. It provides a $2AI_0$ in the output resistive load when the duty cycle is 0.5.

In a static converter, passive and active components are subjected to constraints whose magnitude depends on the transmitted power. The technology, as well as the materials constituting those components affects the ideal operating mechanisms leading to the emission of high level EM interferences. Sometimes, the theoretical operating mode of all the structure itself may be compromised. The parasitic components which contribute significantly to the disturbances (radiated and conducted) are represented in the electrical circuit of the converter (Fig. 3) as located components (stray inductances and stray capacitances).

With: l_e : Intrinsic inductance of the input capacitor, l_c : Inherent inductance of the switching cell, C_{DS} : Drain-source junction capacitance, C_{Di} : Diode junction capacitance.

The inductances l_e, l_c have a great influence on the radiated magnetic field. They are proportional to the radiating areas of the converter. The common mode parasitic capacitance C_p is sufficiently small and does not influence the main phenomena due to the switching cell.

4. Frequency identification

For such a device the radiations phenomena are due to the switching frequency and the transient phenomena happening during the commutations. In order to define these frequencies measurements of the z -component of the magnetic field (H_z) have been collected 8 cm above the converter switching cell. Two series of measures have been collected for two different frequency bands: 9–150 kHz and 10–300 MHz. The corresponding spectra are represented on Figs. 4 and 5.

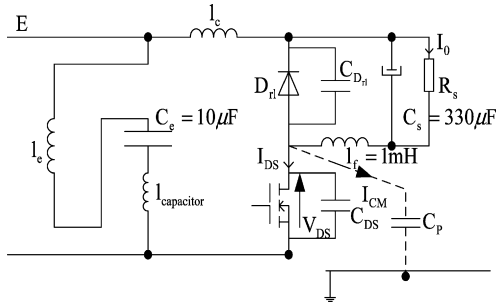
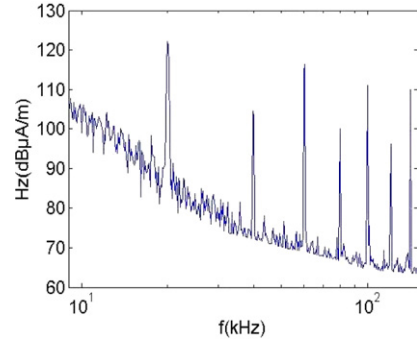
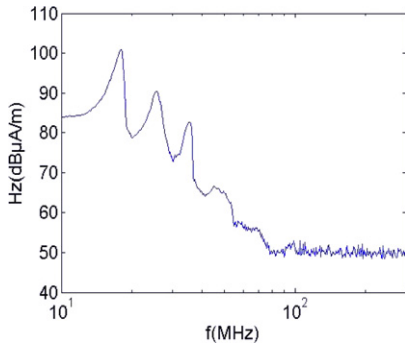
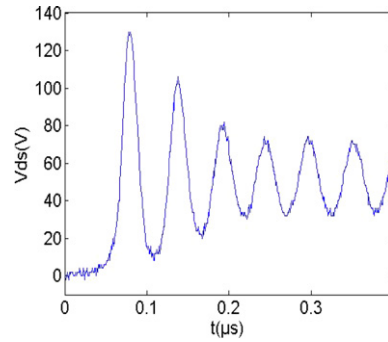


Fig. 3. Electrical circuit of the chopper.

Fig. 4. H_z low-frequencies spectrum (10–150 kHz).Fig. 5. H_z high-frequencies spectrum (1–300 MHz).Fig. 6. Voltage V_{DS} at switching-off, parasitic resonance at 17.9 MHz.

For low frequencies (Fig. 4), the switching frequency and its first harmonic ranks can be identified. The maximum level is obtained for the fundamental (20 kHz). In high frequencies (Fig. 5), two important peaks appear. The first one corresponds to $f_1 = 17.9$ MHz and the second one to $f_2 = 26$ MHz.

A transient phenomenon corresponding to the resonant frequency $f_1 = 17.9$ MHz is observed on the drain-source voltage and the drain-source current at switching-off while the $f_2 = 26$ MHz resonant frequency is observed on both signals at switching-on (Figs. 6 and 7).

Mechanisms of resonant frequencies presented above can be described on two steps as follows:

Step 1: Switching-off. At time $t = \alpha T$, the MOSFET is switched-off, so the current I_{DS} begins to fall and the diode D_H is now conducting. A resonant transient occurs involving the parasitic elements of the switching cell. The evolution of the quantities V_T and I_{DS} are described by the following expressions:

$$\begin{aligned} V_T &= E[1 - \cos(w_{HF}t) \exp(-\zeta w_{HF}t)] \\ I_{DS} &= E \sqrt{\frac{C_{DS}}{l}} [\sin(w_{HF}t) + \zeta \cos(w_{HF}t)] e^{(-\zeta w_{HF}t)} \end{aligned} \quad (11)$$

where ζ is the damping factor of the switching cell and:

$$w_{HF} = \frac{1}{\sqrt{l C_{DS}}} \quad (12)$$

This step ends when: $V_k = E$.

Step 2: Switching-on. At time $t = 0$, the MOSFET is switched-on. So the current I_{DS} is growing until diode D_H is locked.

The same resonant phenomenon occurs in the switching cell involving the same parasitic inductance with D_H junction capacitance. Then, the resonant frequency is $f_2 = 26$ MHz.

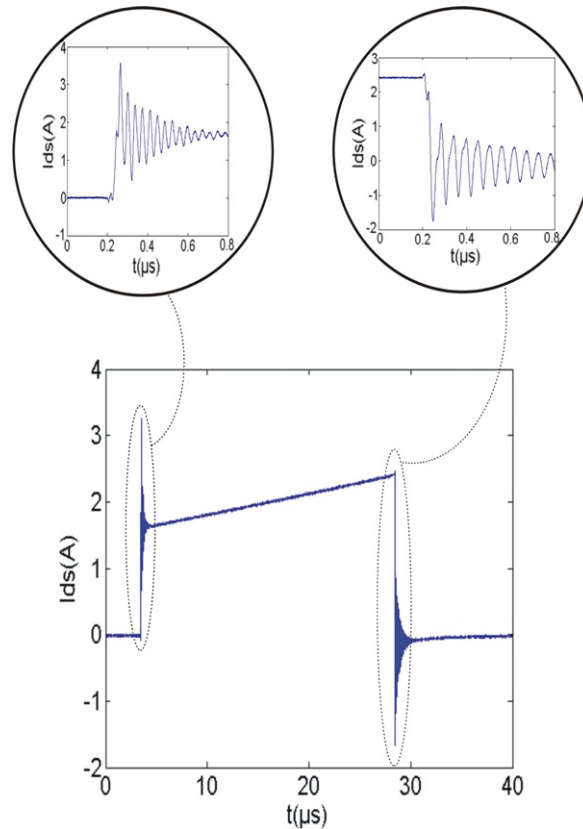


Fig. 7. Current I_{ds} waveform, switching-on and switching-off.

Table 1
Parameters of the model magnetic dipoles.

Dipole	X (cm)	Y (cm)	M ($A\ m^2$)	U_x	U_y	U_z
1	7.5	3	0.0026	0.09	-0.3	-0.92
2	14.5	4.5	0.0038	0.03	0	-0.99

It can be said that the magnetic field emission in high-frequency (far from the switching frequency) is mainly caused by the di/dt and dv/dt during the switching transients of the transistor, in the switching cell. As a first conclusion it can be said that for the converter, low- and high-frequency radiating sources are the same since they involve the same parts of the electric circuit.

5. Results

The efficiency of the identification method has been tested on the Buck chopper. The reflexion phenomena due to metallic ground plane (heat sink) situated under the electric circuit, are taken into account using the image theory.

Since the radiating sources are the same for low- and high-frequencies, the results are presented only on the switching frequency (20 kHz). The characterization method shows that the Buck chopper can be efficiently represented by two magnetic dipoles whose parameters are presented in Table 1.

According to the magnetic field cartographies we can say that a good agreement between the measured field and the theoretical values is obtained (see Fig. 8).

The 3D aspect of the model is shown on Fig. 9 where a superposition of the model results with the real sources on the PCB is illustrated. The dipoles distribution (position and moment orientation) is very close to that of the real sources resulting from the current distribution in the electric circuit.

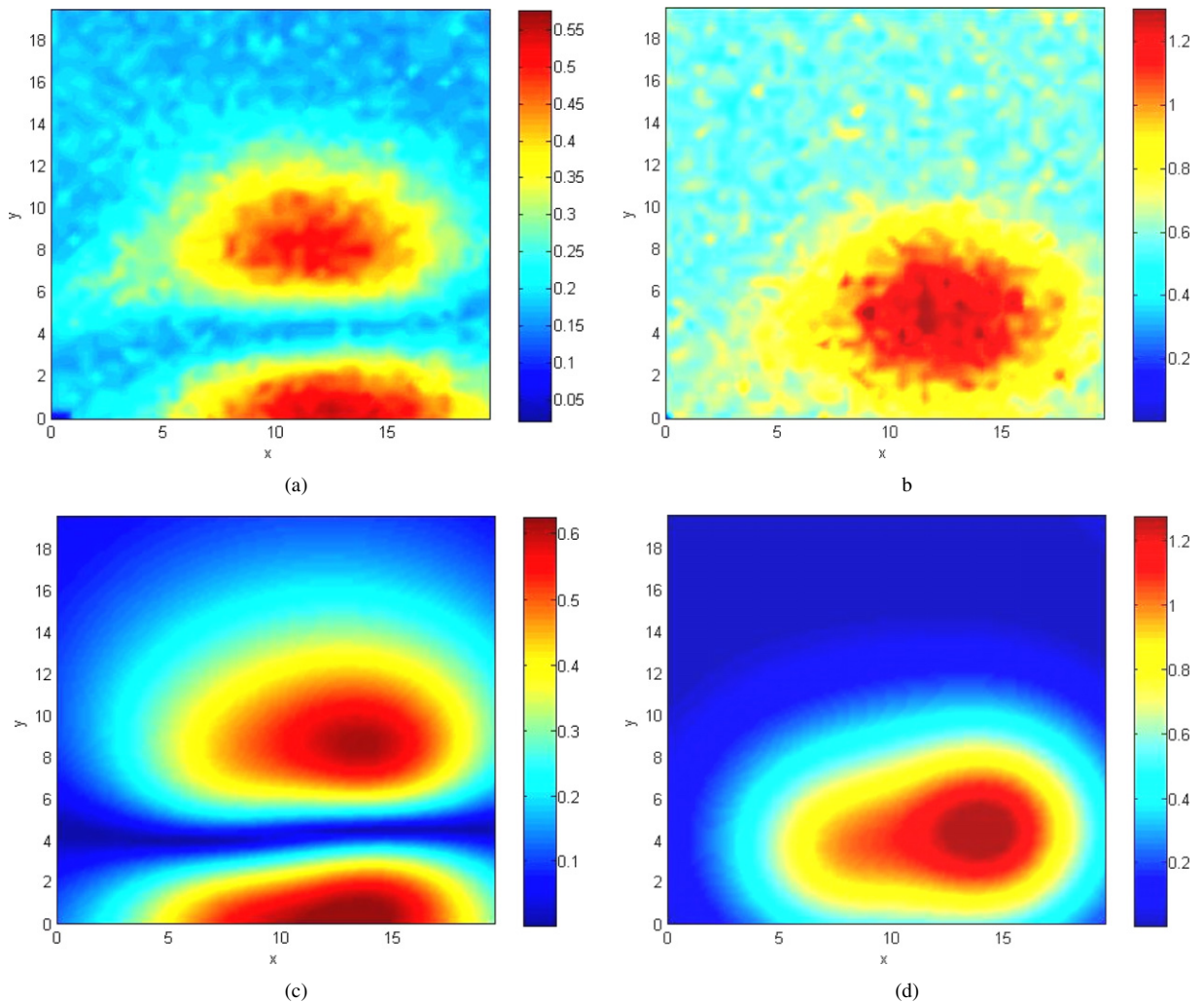


Fig. 8. (a) Measured and (b) theoretical magnetic field H_y ($A m^{-1}$); (c) Measured and (d) theoretical magnetic field H_z ($A m^{-1}$).

Changing the switching frequency will change the values of the currents in the circuit and therefore the moment amplitude of the sources. However, the geometric parameters (position, size of the dipoles and the orientation) are still the same. Then we have to deal only with one parameter for each dipole instead of six.

6. Conclusion

In this article a characterization method of radiated emissions from power electronic devices has been presented. It is an inverse problem-based resolution method. This method allows replacing the real system by a 3D behavioural model using near-field measurements obtained on a test bench. The model consists in a set of elemental magnetic dipoles whose position as well as moment amplitude and moment orientation are found by minimizing a fitness function using a genetic algorithm.

The efficiency of this method has been tested on an academic Buck chopper: the results obtained with this method are very close to measurements, and satisfy the goals of the study. The simple expressions of the fields radiated by the dipoles allow an easy prediction of the far-field if needed. Such an approach provides a useful tool in order to evaluate the impact of the power system on other electronic circuits located nearby, and to find efficient solutions if the reduction of the radiated field is needed.

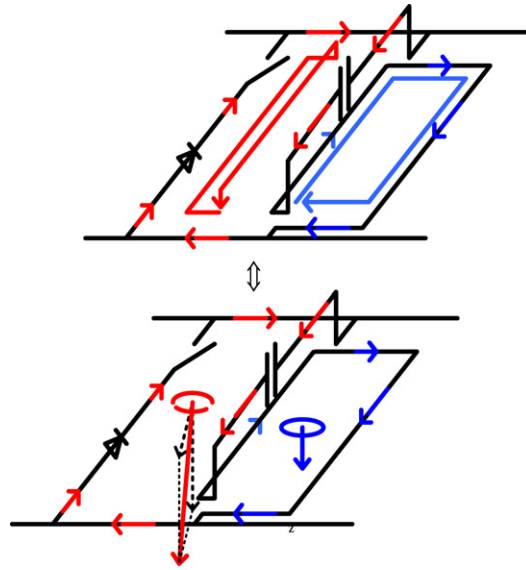


Fig. 9. Comparison between real sources and electromagnetic model.

Acknowledgements

The authors acknowledge Cécile Labarre and Ouafae Aouine from École des mines de Douai for providing the relevant experimental results in the power converter used in this study.

References

- [1] O. Aouine, et al., Measurements and modeling of the magnetic near field radiated by a Buck chopper, *IEEE Transactions on Electromagnetic Compatibility* 50 (2008) 445–449.
- [2] J. Vives-Gilabert, et al., Modeling magnetic radiations of electronic circuits using near-field scanning method, *IEEE Transactions on Electromagnetic Compatibility* 49 (2007) 391–400.
- [3] J.-R. Regué, et al., A genetic algorithm based method for source identification and far-field radiated emissions prediction from near-field measurements for PCB characterization, *IEEE Transactions on Electromagnetic Compatibility* 43 (2001) 520–530.
- [4] E. Roubine, J. Bolomey, *Antennes ; 1 – Introduction Générale*, Masson, Paris, 1977.
- [5] Z. Michalewicz, *Genetic Algorithms + Data Structures = Evolution Programs*, third, revised and extended edition, Springer, 1996.